Available online at www.sciencedirect.com
SCIENCE DIRECT
Journal of the European Ceramic Society 26 (2006) 2389–2396
www.elsevier.com/locate/jeurceramsoc

Modelling silicon carbide formation during heating at constant rate

A. Lemarchand[a,b,*], J.P. Bonnet[b,c]

[a] *Université Pierre et Marie Curie, Laboratoire de Physique Théorique des Liquides, C.N.R.S. U.M.R. 7600, 4, place Jussieu, case courrier 142, 75252 Paris Cedex 05, France*
[b] *GDR 2391 SC CNRS, Groupe Français d'autocombustion, France*
[c] *Ecole Nationale Supérieure de Céramique Industrielle, Groupe d'étude des Matériaux Hétérogènes, E.A. 3178, 47-73, avenue Albert Thomas, 87065 Limoges, France*

Received 28 November 2004; received in revised form 23 March 2005; accepted 9 April 2005
Available online 31 May 2005

Abstract

We build a model, at a mesoscopic, nanometric scale, describing the formation of silicon carbide during heating at constant rate followed by holding at a temperature slightly smaller than the eutectic temperature of carbon and silicon. The number of contacts between silicon grains and graphite plates in the initial powder mixture is shown to influence the speed of the reaction during the step associated with the melting of silicon. After dissolution of carbon in liquid silicon, precipitation of silicon carbide is assumed to obey a heterogeneous nucleation mechanism. In agreement with experiments, the simulation results reproduce smaller reaction speeds for larger silicon grains.

Keywords: Powders-solid state reaction; SiC; Grain size; Grain growth; Porosity

1. Introduction

Mechanically-activated [1] or field-assisted [2] syntheses, reactive waves in multilayer nanofilms [3], synthesis of nanostructured materials [4], and controlled welding under pressure [5] are some promising experimental directions in order to produce new nanomaterials hardly obtained by classical routes. Nevertheless, the control of heterogeneous high-temperature reactions [6] remains a challenge and the main preoccupation is the understanding of the underlying mechanisms, in order to produce materials with predefinite microstructure and porosity. Short time of reaction, existence of structure transformations as well as high temperature make difficult direct in situ observations of the processes. Almost nothing is known about synthesis in nano-scale systems, with characteristic size of reactant powder less than 100 nm. For powders with grains of micrometric size, most of well-known reference data concerning reaction mechanisms in heterogeneous reactions have been analyzed at a macroscopic scale [7–9]. Uniformity of the mixture is usually assumed in planes perpendicular to the direction of propagation of the reaction front and some parameters controlling the geometry of the grains are introduced in the partial differential equations for macroscopic variables like temperature and reaction extent [10,11]. In parallel with the development of new experimental methods, including time-resolved X-ray diffraction [12] using synchrotron radiation, the development of theoretical models at a mesoscopic scale is required.

In this paper we focus on modelling the formation of silicon carbide, SiC, during heating at constant rate until a temperature slightly smaller than the eutectic temperature of carbon and silicon, $T_e = 1404\,^{\circ}C$. Our goal is to build a minimal model capturing the essential features of the phenomenon. We wish to extract from the experimental results [13] the elementary processes that control the reaction. The number of parameters is too large to perform series of experiments in order to extract by trial and error their effects on the resulting materials. It is more efficient to build a model, valid at a mesoscopic scale and relying on well-identified hypotheses, easy to check and possibly to reject. Fig. 1 shows the experimental results [13] observed when mixtures of carbon and silicon

* Corresponding author. +33 1 44 27 72 92; fax: +33 1 44 27 72 87.
E-mail address: anle@lptl.jussieu.fr (A. Lemarchand).

0955-2219/$ – see front matter © 2005 Elsevier Ltd. All rights reserved.
doi:10.1016/j.jeurceramsoc.2005.04.012

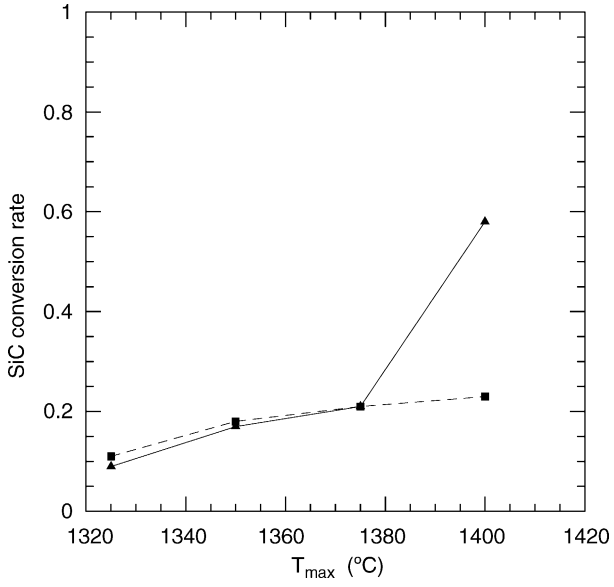

Fig. 1. Experimental conversion rate in silicon carbide vs. maximal temperature reached during heating at constant rate (15 °C min^{-1}) followed by immediate cooling [13]. Carbon and silicon were in a molar ratio of 1.1. The porosity of the inital mixture was 50%. The powder of carbon used was natural graphite (Alfa Aesar) with $d_{50} = 10.5$ μm, i.e. such that 50% of the mass of carbon consists of grains of diameter smaller than 10.5 μm. The triangles give the results obtained for small silicon grains (Fluka) with $d_{50} = 5.7$ μm. The squares are obtained for larger silicon grains (Fluka) with $d_{50} = 33.9$ μm. The solid and dashed lines are a guide for the eyes.

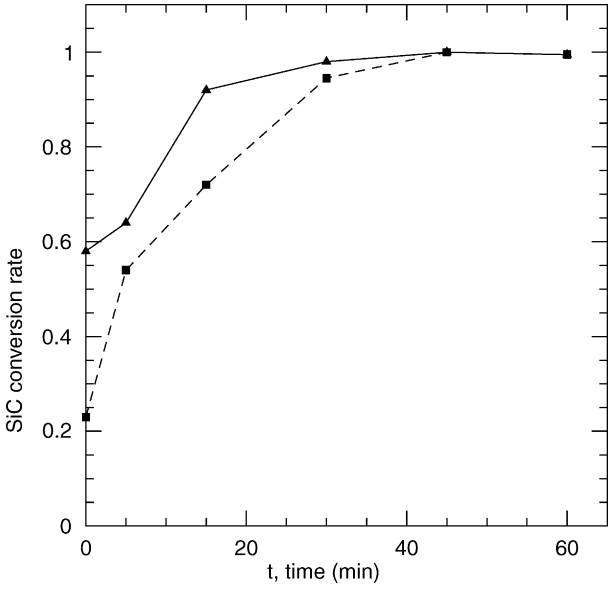

Fig. 2. Experimental conversion rate in silicon carbide vs. time [13] during holding at 1400 °C and after a preliminary temperature ramp of 15 °C min^{-1}. The powders are the same as in Fig. 1.

powders are brought at constant rate up to a maximal temperature ranging between 1325 and 1400 °C; the samples are then immediately cooled. The percentage of silicon carbide formed increases with the maximal temperature reached. Fig. 2 gives the evolution of SiC conversion rate [13] during holding at 1400 °C. The maximal temperature reached after heating at constant rate can be identified with time. Using Figs. 1 and 2, we give in Fig. 3 the qualitative evolution of the extent of the reaction during heating up to 1400 °C and holding at 1400 °C. Three different domains are obtained: a fast regime II is observed between two slow regimes, I and III. The experiments prove that the speed of the reaction in the fast regime II sensitively depends on the size of silicon grains. We wish to check if this stage of the formation of silicon carbide is controlled by the number of solid–solid contacts between carbon and silicon as proposed by Pampuch and co-workers [14–16]. The slow regimes, I and III, observed at the beginning and at the end of the reaction, are nearly independent of the silicon grain size and we ignore these stages in the following.

Our first concern is the simulation of grain distribution in the initial mixture of silicon and graphite. To simulate mixtures of powders at a mesoscopic scale, we admit that graphite grains are comparable to plates and silicon grains to spheres, as shown in the electronic microscopy images given in Figs. 4 and 5. Typically the spatial resolution chosen is the width of the graphite plates, of the order of 100 nm. We first determine the variation of the number of contacts between carbon and silicon with the radius of silicon grains. We then build a simulation model, based on experimental results and reproducing the formation of SiC from these contact sites.

Silicon carbide formation is assumed to obey a heterogeneous nucleation mechanism. We conjecture that the transition between domains I and II shown in Fig. 3 occurs when silicon begins to melt locally, around the sites where the exothermic formation of SiC occurs. The experimental results evidence the contribution of a dissolution–precipitation

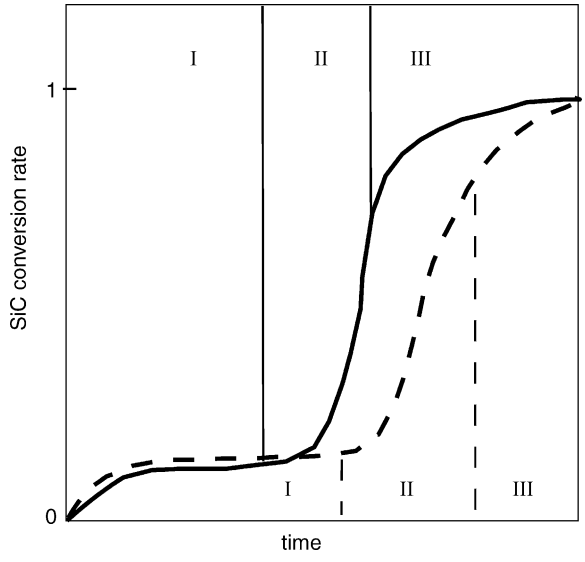

Fig. 3. Expected variation of SiC conversion rate vs. time for an equimolar mixture of silicon and carbon during heating at constant rate and holding at a temperature slightly smaller than $T_e = 1404$ °C. Solid line corresponds to smaller Si grains than dashed line, for identical carbon grains. A fast regime II between two slow regimes, I and III, is identified. The limits between the different domains are drawn at the top of the figure for the small Si grains and at the bottom, for the larger grains.

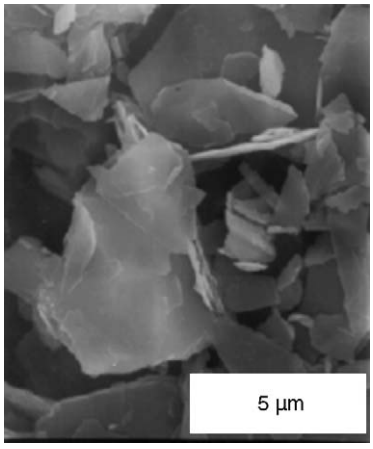

Fig. 4. Electronic microscopy image of natural graphite powder (Alpha) used in the experiments. Grains look like plates of long side equal to $l_c = 7.9\,\mu m$ in average.

mechanism [16,17]. Carbon dissolves in liquid silicon and silicon carbide precipitates mostly at the interfaces between liquid silicon and a solid. As long as solid silicon sites remain, we admit that the heat release accompanying the exothermic creation of a SiC site is entirely used to melt some silicon sites. The experiments shown in Fig. 2 do not reveal a thermal explosion and the silicon carbide obtained does not result from a self-propagating high-temperature synthesis (SHS) procedure. Even during the fast regime, the reaction remains sufficiently slow to allow for a rapid homogenization and relaxation of temperature toward the equilibrium value. In the simulation, we suppose that the temperature of the mixture is fixed at the eutectic temperature of the mixture carbon-silicon, T_e, and we ignore its evolution.

We present in Section 2 the method used to simulate the initial mixture of carbon and silicon. We build in Section 3 a model adapted to the description of the fast regime before the entire melting of silicon. The variation of the extent of reaction as a function of the size of silicon grains is compared to experimental results. Section 4 is devoted to conclusion.

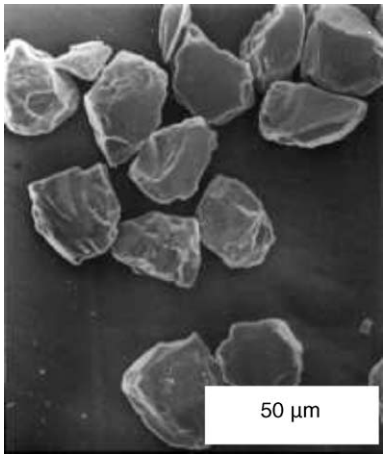

Fig. 5. Electronic microscopy image of a silicon powder (Fluka) used in the experiments. Grains look like spheres of mean radius $r = 17\,\mu m$.

2. Number of contacts between carbon and silicon grains in the initial mixture of reagents

We first explain how we generate the initial mixture of reactive powders, described at a mesoscopic scale. As shown in Fig. 4, electronic microscopy images of carbon powders reveal that natural graphite assumes flat, facetted shapes. A careful analysis of different photos has shown that carbon grains may be approximate by rectangular plates of characteristic lengths l_c, $l_c/2$ and $\Delta l_c \simeq l_c/50$, with l_c in the range $2\,\mu m \leq l_c \leq 25\,\mu m$. According to Fig. 5, silicon grains are more isotropic and may be approximate by spheres of radius r. Two different silicon granulometries have been used with respective average grain radius 2.9 and 17.0 μm. Experiments are carried out for equimolar mixtures of C and Si. We call $\alpha(r)$ the number of carbon plates for one sphere of silicon of radius r such that the resulting three-dimensional (3d) mixture would be equimolar. We simulate a 2d-cut of the mixture and consider carbon segments and silicon disks. For a fixed length l_c, a carbon segment is defined by the two coordinates of one of its tips and by the angle fixing its orientation. For a fixed radius r, a silicon disk is simply defined by the two coordinates of its center.

An initial configuration of a 2d-cut of the mixture of powders is generated as follows. A given number n_s of disks of radius r are generated without overlap in a square box of side $2rf\sqrt{n_s}$ where parameter f controls the relative density of the mixture. A number $n_s\alpha(r)^{2/3}$ of segments of length l_c are generated without overlap. Typically, we choose $n_s = 20$. We have checked that the results are unchanged for $n_s = 10$ and $n_s = 40$. In the simulations the radius of the Si disks is chosen in the range $1.2\,\mu m \leq r \leq 50\,\mu m$, depending on the starting powder granulometry. According to the powder used in the experiments, The length of carbon rods is fixed at $l_c = 7.9\,\mu m$. Fig. 6 gives an example of configuration obtained for large silicon disks with respect to carbon segments. The parameter controlling relative density is fixed at $f = 1.37$ leading to 30% of silicon, 14% of carbon and 56% of pores in volume for the corresponding 3d-mixture. In view of the silicon molar volume and carbon molar volume this composition corresponds to equimolar mixtures and porosity is not very different from the experimental value evaluated at $50\% \pm 1\%$ [18].

Considering a given set of parameters and a given configuration, we determine the fraction $F_{C/Si}$ of carbon segments in contact with a silicon disk. This fraction $F_{C/Si}$ is defined for a given realization of the mixture as the ratio of the number of segments in contact with a disk and the total number of segments $\alpha(r)$. The variation of $F_{C/Si}$ with the radius r of silicon disks is given in Fig. 7. In the range of r-values used in the experiments, $F_{C/Si}$ appears as a monotonically decreasing function of radius r. For purely geometrical reasons, the number of contacts between carbon segments and silicon disks decreases as the disk radius increases. We examine in the next section how this characteristics of the initial mixture may influence the speed of the reaction in the fast regime.

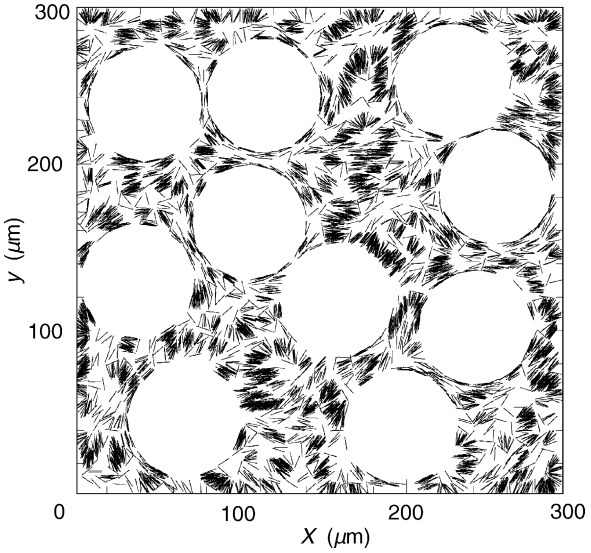

Fig. 6. Initial configuration of a mixture of $n_s = 10$ disks (in white) of radius $r = 33.9\,\mu m$ and $\alpha(r) = 6080$ rods (in black) of length $l_c = 7.9\,\mu m$ mimicing a 2d-cut of an equimolar mixture of silicon grains and graphite plates. The parameter controlling relative density is fixed at $f = 1.37$.

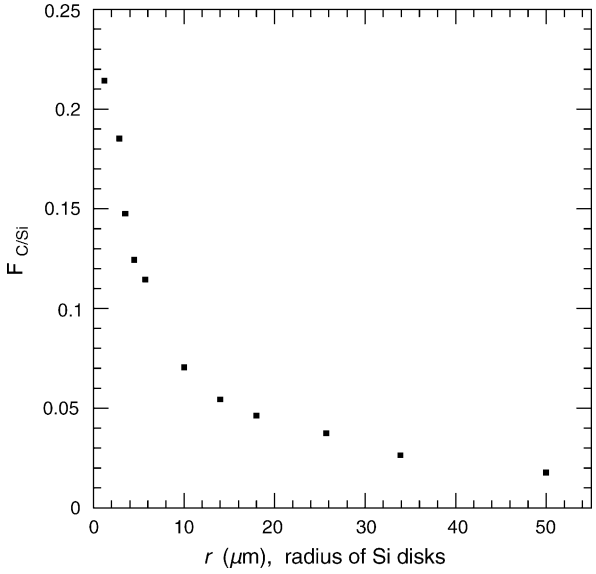

Fig. 7. Fraction $F_{C/Si}$ of carbon segments in contact with a silicon disk as a function of the radius r of the disks. The results are deduced from a realization of a mixture of $n_s = 20$ disks of radius r and $\alpha(r)$ segments of length $l_c = 7.9\,\mu m$. The parameter controlling relative density is fixed at $f = 1.37$.

3. A model for the fast regime

We wish to build a model reproducing experiments[13] where the initial mixture is placed in a furnace, that increases temperature of 15 °C per minute until a maximum value T_{max}, where $T_{max} = 1325\,°C + n25\,°C$ with $n = 0, 1, 2, 3$. The experimental results are given in Fig. 1. Note that T_{max} remains smaller than the temperature of the carbon-silicon eutectic, $T_e = 1404\,°C$. When T_{max} is reached, the sample is immediately cooled and the conversion rate in SiC is deduced from X-ray diffraction patterns.

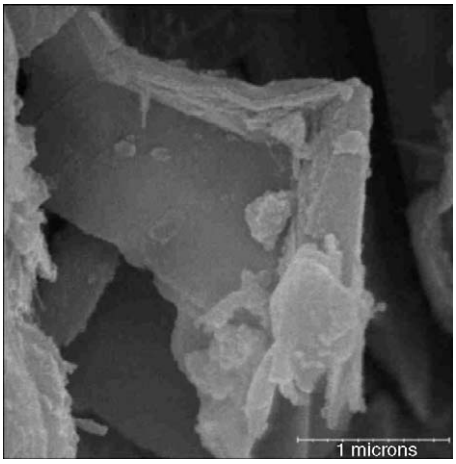

Fig. 8. Electronic microscopy image of the reactive mixture powder brought at $T_{max} = 1375\,°C$ and cooled. The preferential localisation of silicon carbide on the edges of graphite plates can be observed.

For $T_{max} \leq 1375\,°C$, the conversion rate increases slowly and is nearly independent of the size of silicon grains in the initial mixture. This temperature domain defines region I shown in Fig. 3. Whatever the radius r of silicon grains in the range $1.2\,\mu m \leq r \leq 50\,\mu m$, a conversion rate of $21\% \pm 1\%$ has been observed for $T_{max} = 1375\,°C$. As seen in Fig. 8, electronic microscopy images of the samples obtained for $T_{max} = 1375\,°C$ reveal that silicon carbide forms on the edges of the graphite plates that exhibit lateral growth. To explain this preferential localization of SiC, a preliminary mechanism, involving diffusion of silicon on the large plate sections, the (0 0 1) graphitic planes, and nucleation on small sections of higher energy, may be invoked. Indeed, the surface energy of (1 0 0) prismatic planes is known to be higher that the surface energy of graphitic planes[19]. In the simulation model we discard the description of domain I to focus on the step that strongly depends on the size of the silicon grains. As observed in Figs. 1 and 2 for $1375\,°C < T_{max} < 1404\,°C$, the conversion rate becomes highly sensitive to r in the fast regime, i.e. domain II in Fig. 3. In this domain liquid silicon appears thanks to heat release following the formation of silicon carbide. Domain II can be defined as the domain where solid and liquid silicon coexist, so that the temperature of the sample remains close to the eutectic temperature.

3.1. Creation of a layer of potentially liquid silicon around the graphitic skeleton

An initial configuration of the mixture is obtained according to the procedure given in Section 2. Space is then discretized. The minimal length resolution, given by the side of an elementary square site, is chosen equal to the width of the carbon plates, $\Delta l_c = l_c/50$. We define initially four different natures of sites: pores, carbon sites, solid silicon sites, and reactive sites R_c. The latter are defined as solid silicon sites

with a side in common with a carbon site. These reactive sites are the sites of contact between the two reagents. When the reactant powder is brought at a temperature slightly smaller than the eutectic temperature, we assume that the limiting process is the formation of silicon carbide at the interface between graphite and silicon. In other words, we admit that the exothermic reaction

$$\mathrm{Si} + \mathrm{C} \rightarrow \mathrm{SiC} + \mathrm{heat} \tag{1}$$

occurs at contact sites R_c. We define p_c as the probability that a reactive contact site R_c actually reacts during the time step Δt.

The densities and molar masses of silicon and silicon carbide are:

$$\rho_{Si} = 2330\,\mathrm{kg\,m^{-3}}, \qquad M_{Si} = 0.028\,\mathrm{kg\,mol^{-1}}, \tag{2}$$

$$\rho_{SiC} = 3220\,\mathrm{kg\,m^{-3}}, \qquad M_{SiC} = 0.040\,\mathrm{kg\,mol^{-1}}. \tag{3}$$

Consequently, the ratio of the number of moles of silicon and silicon carbide in an identical volume is very close to unity and obeys:

$$\frac{n_{Si}}{n_{SiC}} = \frac{\rho_{Si} M_{SiC}}{\rho_{SiC} M_{Si}} = 1.03. \tag{4}$$

Since reaction (1) leads to the formation of one mole of silicon carbide from 1 mole of silicon, we mimic the reaction by transforming at each time step an appropriate number of reactive silicon sites into the same number of silicon carbide sites. Moreover we neglect the consumption of carbon sites. Denoting $N_{R_c}(0)$ the initial number of reactive sites R_c, we transform a number $p_c N_{R_c}(0)$ of reactive sites into silicon carbide sites during the first time step Δt. Until solid silicon remains, we admit that the heat release following the exothermic reaction (1) is entirely used to melt silicon. The mean number $\bar{x}$ of liquid silicon sites created for each formation of a silicon carbide site is deduced from the ratio of the standard enthalpy of reaction per kilogram of mixture at the eutectic temperature T_e, $\Delta_R H^\circ = -3.424 \times 10^6\,\mathrm{J\,kg^{-1}}$, and the enthalpy of fusion of silicon, $\Delta_f H^\circ = 1.787 \times 10^6\,\mathrm{J\,kg^{-1}}$. As shown in Eq. (4), silicon and silicon carbide have nearly the same molar volume and the two crystals present structural similarities. Neglecting the variation of surface energy accompanying the precipitation of SiC, we have:

$$\Delta_R H^\circ \rho_{SiC} + \bar{x} \Delta_f H^\circ \rho_{Si} = 0 \tag{5}$$

Using the densities of silicon and silicon carbide given in Eqs. (2) and (3), we find:

$$\bar{x} = 2.65. \tag{6}$$

Molten silicon is known to form a liquid of weak viscosity, able to wet the graphite plates. Instead of simulating the movements of liquid silicon and following the evolution of solid silicon sites, we determine the total initial number of solid silicon sites and create a priori an identical number of potentially liquid silicon sites around the skeleton of carbon

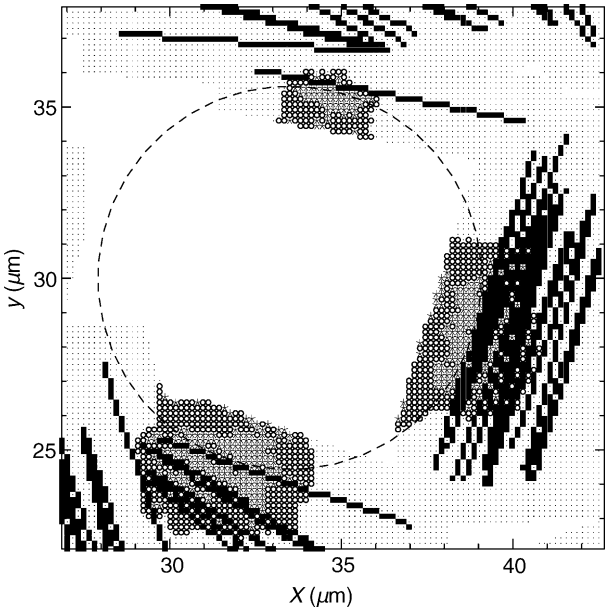

Fig. 9. Detail of a discretized configuration obtained at the beginning of the melting of silicon at time $t = 5$ (arbitrary units) for $n_s = 30$ disks of radius $r = 5.7\,\mu\mathrm{m}$ and $\alpha(r) = 516$ rods of length $l_c = 7.9\,\mu\mathrm{m}$. Parameter controlling relative density: $f = 1.37$, probability of reaction of a (solid or liquid) silicon site in contact with carbon: $p_c = 0.2$, probability of reaction of a liquid silicon site in contact with silicon carbide or solid silicon (whose role is played by pores), $p_s = 0.5$. The dashed circle represents the initial circumference of a solid silicon disk. Black squares: carbon site, open circles: liquid silicon site, star: silicon carbide site, small dots: potentially liquid silicon sites, i.e. empty sites surrounding the carbon rods that would be occupied by liquid silicon after melting of all silicon sites.

rods. A detail of the liquid layer, that would cover the carbon segments if all silicon was melted, can be seen in Fig. 9. After entire melting, the place occupied by a disk of solid silicon would be replaced by liquid silicon and a pore of smaller radius. After the formation of each new SiC site, 2 or 3 potentially liquid silicon sites, in the closest possible neighborhood of the SiC site formed, are transformed into actually liquid Si sites.

3.2. Simulation of the precipitation of silicon carbide

Silicon carbide is assumed to form according to a dissolution–precipitation mechanism [16,17]. As far as liquid silicon and carbon remains in contact, carbon dissolves in liquid silicon. The composition of the eutectic corresponds to 98.5% of silicon for 1.5% of carbon. We admit that the precipitation of silicon carbide follows a heterogeneous nucleation mechanism. Contrary to the case of homogeneous nucleation, the grains of SiC formed never disappear, whatever their size. Moreover, crystallisation preferentially occurs at a solid–liquid interface. As soon as reaction has begun, liquid silicon may be in contact with 3 different solids: carbon, solid silicon or silicon carbide. Consequently the notion of reactive sites has to be extended. The sites R_c of contact between Si and C are not only the initial solid silicon sites in contact with carbon but also the liquid Si sites with a side in

common with a carbon site. All these contact sites R_c react with the same probability p_c.

As already mentioned, the cristallographic nature of Si and SiC surfaces can be rather similar for some specific crystallographic orientations. Therefore, we can consider that their behavior are close and we only introduce a second type of reactive sites, denoted R_s, defined as the liquid Si sites with a side in common with a solid silicon site or a silicon carbide site. Since the evolution of solid Si is not taken into account in the simulation, the role of solid Si grains is played by the potential pores that would be created by the entire melting of Si. The reactive sites R_s react with a probability p_s. We assume that (i) temperature is fixed at the eutectic temperature T_e, (ii) formed silicon carbide does not block the contact between carbon and liquid silicon. Hence, the percentage of carbon dissolved in liquid silicon is fixed at the eutectic composition and the probability p_s keeps a constant value. We have chosen a larger value for p_s than for p_c to reproduce the preferential precipitation of silicon carbide on Si and SiC surfaces than on graphite surface. We show in the following that the results are not very sensitive to the values of p_s and p_c.

Denoting respectively $N_{R_c}(t)$ and $N_{R_s}(t)$ the numbers of reactive sites R_c and R_s at a given time t, the simulation procedure is the following: randomly chosen $p_c N_{R_c}(t)$ reactives sites R_c and $p_s N_{R_s}(t)$ reactives sites R_s are transformed into SiC sites. For each formation of a new SiC site, we form either $x = 3$ or $x = 2$ liquid Si sites depending on wether $x(t)$, defined as the average of x computed from $t = 0$, is smaller or larger than $\bar{x} = 2.65$. Hence, $x(t)$ slightly fluctuates around the correct mean value. According to the nature of the neighbors of the liquid Si sites formed, the latter are labelled as reactive sites R_c, R_s, or nonreactive liquid Si sites. Time is incremented by Δt and the same procedure is repeated at $t + \Delta t$. The time units are arbitrary. The allocation of physical values to Δt would require the knowledge of the activation energy of reaction. The simulation is valid when liquid silicon has appeared and until (i) silicon is not entirely melted so that temperature is fixed, (ii) the number of reactive sites R_c does not vanish, so that carbon may dissolve in liquid silicon.

3.3. Comparison of the simulation results with the experiments

Fig. 9 illustrates the beginning of the fast reaction around a silicon disk of the initial mixture. We observe the formation of large grains of SiC by nucleation around the germs located at the initial contacts between solid Si and C. The precipitation of isolated small grains of SiC is also observed at the interface between solid and liquid silicon whose role is played by the interface between pores and liquid silicon.

We give in Fig. 10 the evolution of the extent of reaction $\xi(t)$, for different values of the radius r of silicon disks. The instantaneous value of the extent of reaction (1) is defined as the ratio of the number of silicon carbide sites formed at time t and the initial number of solid silicon sites. The main result

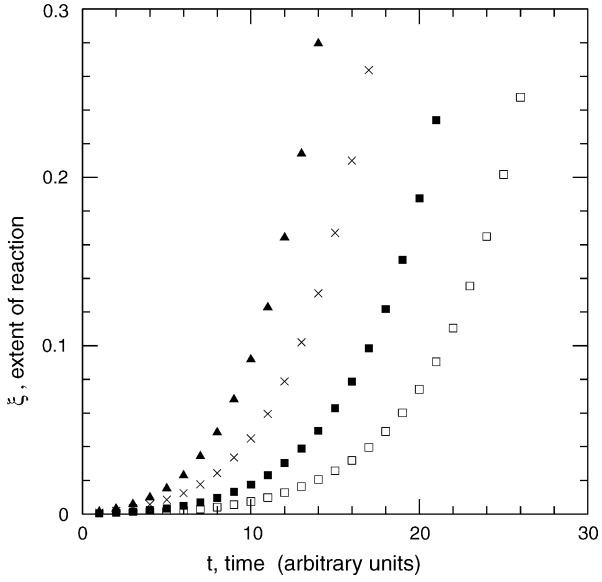

Fig. 10. Time evolution of the extent of the reaction, ξ, for different radii of the disks. Triangles: $n_s = 60$ disks of radius $r = 2.9\,\mu m$, crosses: $n_s = 30$ disks of radius $r = 5.7\,\mu m$, solid squares: $n_s = 20$ disks of radius $r = 17\,\mu m$, open squares: $n_s = 10$ disks of radius $r = 33.9\,\mu m$. The length of carbon rods is fixed at $l_c = 7.9\,\mu m$. Parameter controlling relative density: $f = 1.37$, probability of reaction of a (solid or liquid) silicon site in contact with carbon: $p_c = 0.2$, probability of reaction of a liquid silicon site in contact with silicon carbide or solid silicon, $p_s = 0.5$.

is that reaction is faster for smaller radius of silicon disks. As shown in Table 1, the extent of reaction $\xi(t)$ at a given instant t essentially varies with r in the same proportions as the initial number of contacts between carbon and silicon. In addition to the results of Table 1, the simulation results yield $F_{C/Si} = 0.115$ and $\xi(t = 14) = 0.125$, for $r = 5.7\,\mu m$. Similarly, we obtain $F_{C/Si} = 0.026$ and $\xi(t = 14) = 0.020$, for $r = 33.9\,\mu m$. More generally the ratio of the extents of reaction associated with two different values of r is close to the ratio of the corresponding initial fractions of carbon segments in contact with silicon.

We wish to compare the simulation results with the experimental percentages of SiC. Let us recall the experimental procedure: the initial mixture of Si and C is put in a furnace whose temperature slowly increases until T_{max}, smaller than the eutectic temperature T_e. Then the sample is cooled. The conversion rate is determined from X-ray diffraction patterns of ground powders using the relative intensities of the main peaks of silicon and silicon carbide, and an abacus [13]. For $T_{max} \leq 1375\,^{\circ}C$ the conversion rate does not depend on the radius r of silicon grains. According to the results given in Table 1, the conversion rate reaches 21% for $T_{max} = 1375\,^{\circ}C$, whatever the radius r. Up to $T_{max} = 1375\,^{\circ}C$, the main mechanism involves crystallisation of SiC on the edges of the carbon plates via a mechanism different from that considered here [13]. A completely different behavior is observed for $T_{max} = 1400\,^{\circ}C$, where the conversion rate crucially depends on the radius r and where electronic microscopiy images of the samples reveal the formation of SiC all around the carbon

Table 1
Comparison of the initial fraction $F_{C/Si}$ of carbon segments in contact with a silicon disk, extent of reaction ξ at time $t = 14$ (arbitrary units), experimental values of conversion rates in SiC for $T_{max} = 1375$ and 1400 °C, evaluation of SiC conversion rate between 1375 and 1400 °C for the two different radii of silicon grains used in the experiments

r (μm)	$F_{C/Si}$	$\xi(t = 14)$	Experimental SiC conversion rate for $T_{max} = 1375$ °C	Experimental SiC conversion rate for $T_{max} = 1400$ °C	SiC conversion rate between 1375 °C and 1400 °C
2.9	0.185	0.280	0.21	0.58	0.37
17.0	0.051	0.050	0.21	0.23	0.02

The parameter values of the simulations are the same as in Fig. 10.

plates. We assumed that this transition corresponds to the beginning of the melting of silicon and the simulation results reproduce the period during which solid and liquid silicon coexists. If we subtract the 21% of SiC formed at $T_{max} = 1375$ °C to the conversion rate measured for $T_{max} = 1400$ ° C, we deduce from the experiments that only 2% of SiC forms between 1375 °C and 1400 °C for a large silicon radius $r = 17$ μm, whereas 37% of SiC appears for the small radius $r = 2.9$ μm. The values of the extent of reaction ξ deduced from the simulations are in qualititative agreement with these percentages.

However, the experiments exhibit a larger variation of $\xi(t)$ with r than the simulation results obtained for $p_c = 0.2$ and $p_s = 0.5$. In order to check if a better quantitative agreement with the experiments could be obtained, we have studied the variation of the extent with r for various values of the ratio p_c/p_s at constant sum $p_c + p_s = 0.7$. No significant variation of the ratio $\xi(r = 2.9\,\mu m)/(\xi = 17.0\,\mu m)$ of the extents, at arbitrary time $t = 14$, for $r = 2.9$ μm and $r = 17.0$ μm have been detected when favoring either the direct formation of SiC at the interface between liquid silicon and carbon ($p_c/p_s > 1$), or the precipitation of SiC at the interface between liquid and solid silicon ($p_c/p_s < 1$). We obtain $\xi(r = 2.9\,\mu m)/\xi(r = 17.0\,\mu m) = 5.5 \pm 0.5$ in the whole range $0.1 \leq p_c/p_s \leq 10$.

The successful comparison between the experimental percentages of SiC and the predictions of the simulations can be viewed as a validation of the hypotheses on which the model relies: When the mixture of powders is brought at a temperature slightly smaller than the eutectic temperature, the exothermic formation of SiC around privileged sites, the contact sites between Si and C, leads to the melting of silicon. Then the reaction speed is strongly influenced by the size r of silicon grains. During this stage of the reaction, the dynamics remains correlated to the initial number of contacts between reagents.

4. Conclusion

Simulating a 2d cut of a mixture of silicon grains and carbon plates at a mesoscopic, submicrometric scale, we have shown that the number of contacts between carbon and silicon decreases when the radius of Si grains increases in the range of radii used in the experiments. The evolution of the reactive system during heating and holding at a temperature smaller than the eutectic temperature is simulated in the period associated with the melting of silicon. The model essentially relies on the following hypotheses. A dissolution–precipitation mechanism is assumed with heterogeneous nucleation of SiC at the interfaces between liquid silicon and a solid. The local heat release accompanying the formation of SiC leads to the melting of silicon in the neighborhood of the site where reaction took place. Temperature remains constant until solid silicon is present. Knowing simply geometrical properties of the initial mixture is sufficient to predict the qualitative behavior of the reaction speed as the size of silicon grains varies: The reaction becomes faster when the radius of silicon grains decreases, due to the increase of contacts between reagents. The qualitative agreement between the experimental conversion rate and the extent of reaction deduced from the simulation substantiates the hypotheses.

References

1. Gauthier, V., Bernard, F., Gaffet, E., Josse, C. and Larpin, J. -P., Combining XRD and EXAFS with on-line catalytic studies for in situ characterization of catalysts. *Mater. Sci. Eng. A*, 1999, **272**, 334–341.
2. Charlot, F., Gaffet, E., Bernard, F. and Munir, Z. A., One step synthesis and consolidation of nanophase iron aluminide. *J. Am. Ceram. Soc.*, 2001, **84**, 910–914.
3. Grigoryan, A. E., Elistratov, N. G., Kovalev, D. Yu., Merzhanov, A. G., Nosyrev, A. N., Ponomarev, V. I. *et al*., Autowave propagation of exothermic reactions in Ti–Al thin multilayer films. *Dokl. Phys. Chem.*, 2001, **381**, 283–287.
4. Sytschev, A. E. and Merzhanov, A. G., Self-propagating high-temperature synthesis of nanomaterials. *Russian Chem. Rev.*, 2004, **73**, 147–159.
5. Pascal, C., Marin-Ayral, R. M., Tédenac, J. -C. and Merlet, C., Combustion synthesis: a new route for repair of gas turbine components-principles and metallurgical structure in the NiAl/RBD61/superalloy junction. *Mater. Sci. Eng. A*, 2003, **341**, 144–151.
6. Merzhanov, A. G., SHS technology. *Adv. Mater.*, 1992, **4**, 294–295.
7. Munir, Z. A. and Anselmi-Tamburini, U., Self-propagating exothermic reactions: the synthesis of high-temperature materials by combustion. *Mater. Sci. Rep.*, 1989, **3**, 277–365.
8. Rogachev, A. S., Khomenko, I. O., Varma, A., Merzhanov, A. G. and Ponomarev, V. I., Mechanism of self-propagating high-temperature synthesis of nickel aluminides (part2): crystal structure formation in combustion wave. *Int. J. SHS.*, 1994, **3**, 239–252.
9. Varma, A., Mukasyan, A. S. and Hwang, S., Dynamics of self-propagating reactions in heterogeneous media: experiments and model. *Chem. Eng. Sci.*, 2001, **56**, 1459–1466.
10. Rudnik, T., Lis, J., Pampuch, R., Lihrmann, J.-M. and Stobierski, L., Parameters of the bed of reactants and solid combustion in the Si–C system. *Arch. Combust.*, 1996, **16**, 3–12.

11. Khina, B. B., Formanek, B. and Solpan, I., Limits of applicability of the diffusion-controlled product growth kinetic approach to modeling SHS. *Physica B*, 2005, **355**, 14–31.
12. Bernard, F., Paris, S., Vrel, D., Gailhanou, M., Gachon, J.C. and Gaffet, E., Time-resolved XRD experiments adapted to SHS reactions. Autoreview. *Int. J. SHS*, 2002, **11**, 181–190.
13. Morançais, A., *Porous SiC ceramics obtained by reaction between silicon and graphite: influence of self-propagating reactions on porosity*. Ph.D. thesis, Université de Limoges, France, unpublished, 2002.
14. Pampuch, R., Bialoskorski, J. and Walasek, E., Mechanisms of reactions in the Si + C system and the self-propagating high-temperature synthesis of silicon carbide. *Ceram. Int.*, 1987, **13**, 63–68.
15. Pampuch, R. and Stobierski, L., Solid combustion synthesis of β SiC powders. *Mat. Res. Bull.*, 1987, **22**, 1225–1231.
16. Lis, J., Pampuch, R. and Stobierski, L., Reactions during SHS in a Ti–Si–C system. *Int. J. SHS*, 1992, **1**, 401–408.
17. Morançais, A., Balhoul-Hourlier, D. and Bonnet, J.-P., Reinforcement of very porous SiC ceramics prepared by SHS by addition of nanometric SiC powder in the reactive compact. *Int. J. SHS*, 2003, **12**, 99–106.
18. Morançais, A., Louvet, F., Smith, D. S. and Bonnet, J.-P., High porosity SiC ceramics prepared via a process involving an SHS stage. *J. Eur. Ceram. Soc.*, 2003, **23**, 1949–1956.
19. Blakslee, O. L., Proctor, D. G., Seldin, E. J., Spence, G. B. and Weng, T., Elastic constants of compression-annealed pyrolytic graphite. *J. Appl. Phys.*, 1970, **41**, 3373–3382.